STRUCTURE OF THE CONCENTRATION BOUNDARY LAYER ON MODELS DURING EROSION BY A HIGH-ENTHALPY AIR FLOW

É. B. Georg and M. I. Yakushin

UDC 532.526

Results of measurements of the concentration distribution for the basic components of the boundary layer are presented, and it is shown that the wall region holds promise for the study of spectral absorption coefficients.

Experiments have been performed on a high-temperature gasdynamic facility using a high-frequency induction discharge in an air stream as a gas heater [1]. The facility is shown diagramatically in Fig. 1, the basic parts being as follows: 1) a radio-frequency generator; 2) the test chamber, separating the discharge channel and the inductive heater 3 from the surrounding atmosphere; 4) a two-axis traverse mechanism; 5) the test model; 6) an extensible tube; 7) a centrifugal fan with smoothly controlled output; 8) a bank of flowmeters in the gas output channel; 9) a screw-type air compressor; 10) bottles of inert gases. The facility ordinarily operates with air from a compressor, creating an excess pressure of 0.25 atm. Argon is used to expedite starting of the facility, and the system is switched to the bottles. The source of electrical energy for the induction discharge is a vacuum-tube oscillator, operating at 17 MHz. The maximum usable oscillatory power is 50 kW. The cylindrical discharge channel is a quartz tube containing a two-turn copper solenoid as the inductive heating element.

The gas stream comes to the discharge channel from the forechamber, where it is given a spiral-translational motion. The forechamber has a shaped annular cavity into which the gas is supplied tangentially. Depending on the degree of swirl of the primary gas, three gasdynamic discharge regimes are observed. The optimum regime occurs when the discharge region is filled with hot gas, the discharge ignites from the wall, and the process is not time-limited. In the other cases, for weak gas swirl, the discharge sticks to the wall, which leads to thermal breakdown of the quartz; for severe gas swirl the discharge is drawn upstream, and is finally blown away by the stream of cold gas. The results presented here were obtained with the optimum gasdynamic discharge conditions. A characteristic feature of the process is that the lateral front of the discharge is inclined to the incident flow in such a way that the cold gas flows normally into the "flame" with a velocity $V \sim 0.1$ m·sec^{-1}, is heated, and is accelerated in the axial direction to $V = 30$ m·sec^{-1}.

It is known that the mechanism for obtaining an induction plasma is associated with the existence of induced voltage pulses, and this may be the cause of fluctuations appearing in the plasma. Specially conducted tests have shown that the time interval between the voltage pulses ($t \sim 10^{-8}$ sec) is several orders of magnitude less than the plasma decay time ($t \sim 10^{-1}$ sec). Analysis of high-speed motion pictures shows that there are no brightness fluctuations, i.e., under these experimental conditions the current fluctuations in the inductor do not affect the temperature uniformity of the flow. The radial distribution at the discharge channel exit shows quite an extensive core with constant temperature in the central region, and the variation of axial temperature downstream is typical of laminar flow [2]. On the jet axis, in the working part of the flow, corresponding to the exit of the quartz tube, the hot air temperature is 8500°K, the pressure is 1 kg·cm^{-2}, the electron concentration is $3 \cdot 10^{15}$ cm^{-3}, the total heat flux to the undisturbed cold model is 0.4 kW·cm^{-2}, and the radiative component is 0.1 kW·cm^{-2}. The test models were mounted on a two-axis traverse mechanism, allowing them to be moved inside the jet in the axial and radial directions.

Institute of the Problems of Mechanics, Academy of Sciences of the USSR, Moscow. Translated from Inzhenerno-Fizicheskii Zhurnal, Vol. 32, No. 4, pp. 581-587, April, 1977. Original article submitted May 4, 1976.

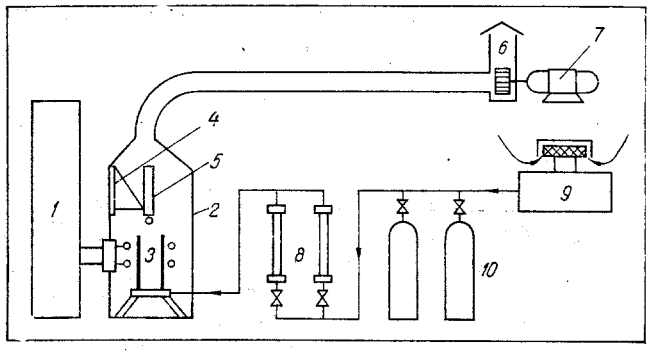

Fig. 1. Optical measurement system.

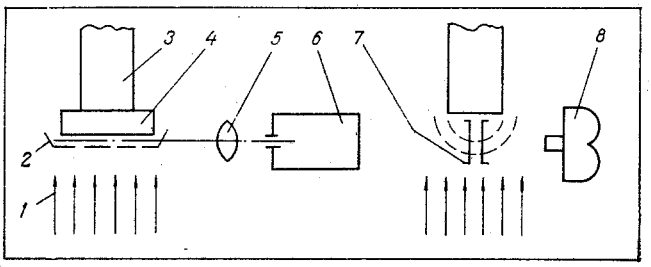

Fig. 2. Optical measurement system.

With flow of the high-temperature gas stream 1 (Fig. 2) the asbestos model 4 forms a boundary layer 2 on its disintegrating surface, consisting of vapors of the material, components of the hot air, and products of reactions between these. The objective of the work is to study the composition of the basic components of the vapor through the boundary layer. In the tests we used flat plate models of width 0.03 m and length 0.035 m, with a cylindrical leading edge of radius 0.015 m. The models were attached to a water-cooled bracket 3, mounted on the traverse mechanism. With a constant-temperature gas flow profile and with two-dimensional models, the conditions in the boundary layer were nearly homogeneous along a generator of the cylindrical model leading edge.

The method of emission spectral analysis was used to study the boundary-layer composition. Figure 2 shows the optical scheme for measuring the radiation of the boundary layer vapor in two planes. The optical scheme, with a magnification of unity, consisted of a standard objective 5 and a type DFS-13 diffraction spectrograph 6 with a plane grating of 1200 lines$\cdot$mm^{-1} and a dispersion of 2 Å$\cdot$mm. The operating width of the grating is 30 μ. The model was focused on the spectrograph slit 7 in such a way that one could simultaneously record the radiation from the boundary layer, the model, and the plasma. Calibration was accomplished by means of a type SI-8-200 standard tungsten lamp. A type IFO-451 recording microphotometer was used for the photographic measurements. The photographic layer blackening was converted into intensity using the heterochromous photometry method. The geometric length of the radiating boundary layer along the line of sight was determined from motion pictures taken with the type KSK-1 camera 8.

The spectral line intensity is the most logical parameter for quantitative evaluation of a boundary-layer element. The physical and chemical processes in the boundary layer generate concentrations of excited molecules, atoms, and ions, which determine the band and line spectral intensities.

We measured the concentrations of the CN radical and of elements from the asbestos decomposition. The measurements of rotational and vibrational temperatures of the CN radical in [3] coincided with ours within the limits of experimental error.

In order to calculate the CN concentration we measured the absolute intensity distribution in the rotational structure of the CN violet band (the 0—1 transition). This intensity can be used as a criterion of CN radical concentration when one is confident that the excitation is due entirely to a thermal mechanism. The radiative intensity of an individual rotational line from the electronic $U \to X$ transition, per unit solid angle, from a layer of length l, is given by the following expression: $I = (16\pi^3/3c^3Z)\nu_{UX}^4 N l \left|R_c^{UX}\right|^2 q_{v'v''} S_{K'K''} \exp \cdot [(-hc/kT)(E_U+E_{v'}+E_{K'})]$.

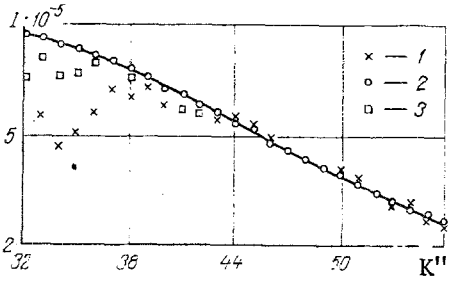

Fig. 3. Distribution of intensity I [W/(cm³•sr)] in the rotational structure of the CH (0 − 1) λ4216-Å band as a function of the rotational quantum number K".

The $|R_e^{UX}|^2$ electron-transition matrix element determines the absolute intensity of the line radiation; the Frank−Condon factor $q_{v'v''}$ describes the intensity distribution in the vibrational structure; and the Hönl−London factor $S_{K'K''}$ determines the intensity distribution in the rotational structure. The quantity $|R_e^{UX}|^2$ has been determined experimentally in [4]. For CN, $|R_e^{UX}|^2 = 0.37$ amu is independent of the internuclear distance and is constant for the entire violet band system. The factors $q_{v'v''}$ and $S_{K'K''}$ were calculated by the methods of quantum mechanics, and $q_{v'v''} = 0.08$ (the 0−1 transition) is given in [5]. The intensity factor for the $^2\Sigma \rightarrow {}^2\Sigma$ transitions for the P and the R branches, $^PS = 2K''$ and $^RS = 2(K'' + 1)$, is given in [6], from which the values of the molecular constants were chosen. The formula was used to determine the CN concentration from the experimentally measured value of individual rotational line intensity. The choice of line is discussed below. Under these conditions ($T \sim 10{,}000°K$), neglect of the induced radiation leads to a negligible error in intensity.

Another factor for which one must consider a correction is self-absorption. The self-absorption was estimated from experimental data. In [3] the relation $\log I = f(K''(K'' - 1))$ was found for all sections of the boundary layer, starting with the inner and finishing at the outer boundary of the vapor. This relation deviates somewhat from a straight line for rotational numbers $K'' \leq 42$. Since we assume that the main effect causing a deviation of the logarithmic intensity dependence $\log I = f(K''(K'' - 1))$ from a straight line is self-absorption, it would be interesting to consider the intensity distribution over the rotational levels for each cross section. By way of example we present a very interesting experimental intensity distribution 1 for the rotational CN structure in the 0−1 band for a single air boundary-layer section with asbestos (Fig. 3). For comparison we present the theoretical relation 2, calculated from the formula on a computer.

In order to obtain the calculated curves for intensity distribution in the rotational structure of the cyanogen band, we wrote a program to determine the temperature and concentration for a given intensity distribution, using experimental values from the lines clearly free of perturbations.

We note that for $K'' \leq 42$ the computed curves lie somewhat above the experimental points, the divergence increasing at each section as the rotational number decreases, and with increase in number of sections the range of these K values and the degree of discrepancy from the theoretical curve decrease.

By comparing the experimental and calculated distributions we were able to find rotational lines with anomalous intensity values; by applying corrections for self-absorption, we obtained the corrected intensity values 3 in Fig. 3.

The concentration was calculated for lines free of overlap, which were found in the P-branch tail with large quantum numbers. Figure 4 shows the variation of CN concentration across the boundary layer for the air−asbestos case. A maximum concentration is clearly seen at a certain distance from the disintegrating wall. The drop in CN concentration as one goes out from the wall begins at a temperature on the order of $T = 4000°K$. It is clear that this is associated with the beginning of CN dissociation, which increases with increase of temperature; the dissociation energy is $E \sim 7.6$ eV [7].

In [8], limiting theoretical CN concentrations were given for the 0−1 band at atmospheric pressure and various temperatures, beginning where the self-absorption effect begins. A comparison with the theoretical data obtained with the theoretical values shows that the self-absorption effect becomes appreciable at distances up to 2.5 mm from the wall. Thus,

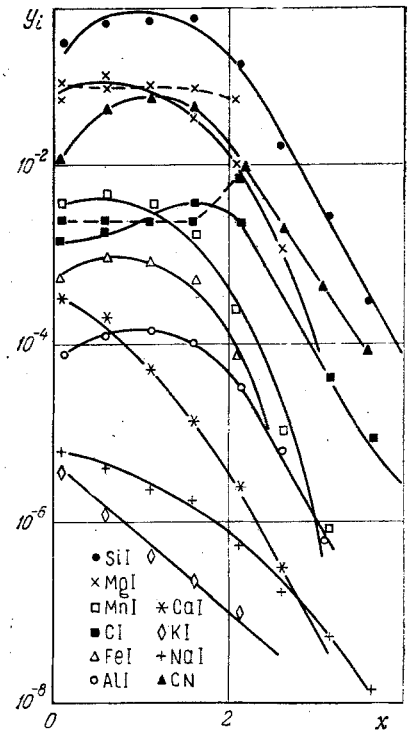

Fig. 4. Profiles of relative concentrations y_i of the boundary-layer vapor, in relative units; x is in mm.

reabsorption is the main factor perturbing the intensity distribution over the rotational levels in the band.

We now estimate the contribution of collision processes and spontaneous transitions of the CN radical. It is known that radiation from small volumes deactivates the excited molecules and atoms. These losses must be compensated for by shock processes. If the collisions are not efficient enough, the distribution of molecules over the excited levels can differ from equilibrium, and temperature measurement gives a low result. The equilibrium level population is established under conditions where the number of excited collisions per second is equal to the number of shocks of the second type, which transfer a radiating molecule from an excited level to a ground level, and we can neglect the number of spontaneous transitions. The efficiency of shock processes in the boundary layer in an air flow can be estimated as follows. For air at temperatures of 3000-8000°K and atmospheric pressure, the number of collisions experienced by the CN radical with molecules of CN, N_2, and CO (the effective cross section for collisions is $Q \sim 4 \cdot 10^{-15}$ cm^2 [4]) is $z \sim 10^{10}$ sec^{-1}. Thus, in a radiative time of $t \sim 10^{-7}$ sec [9], the radical experiences $\sim 10^3$ collisions. Consequently, the collisional processes are dominant.

In determining the atom concentration over a line spectrum we used the well-known formula for the radiative intensity of a spectral line. The values of the characteristic quantity for each line were chosen from the published literature [10-12].

For these measurements it is important to choose the analytical spectral lines correctly. The main criterion in the choice is the composition of the original material, i.e., the concentration of elements constituting a substantial portion of the asbestos. From the viewpoint of the spectral measurements we chose lines free from overlap and also free of noise from more intense neighboring lines. In order to reduce the effect of reabsorption it is advantageous to consider resonance lines with a minimum transition probability for elements whose concentration is appreciable in the original state. In individual cases the effect of self-absorption was checked in radiation from multiplet lines.

In addition, out of the whole set of lines for a given element we considered lines with excitation energy $E_n \leq 5$ eV, in order to eliminate the effect of a hotter side layer on the radiation along the line of sight. Initially we recorded radiative spectra of boundary-layer vapor from disintegrating asbestos in the spectral range 0.2-0.9 μ. From careful analysis of the spectra obtained, taking into account what has been said above, we chose the following spectral lines: 3944 Å, Ci 2478 Å, CaI 6122 Å, CaII 3934 Å, FeI 4375 Å, KI 7665 Å, MgI 4571 Å, MnI 4783 Å, NaI 5890 Å, and SiI 3905 Å.

Figure 4 shows the measured results for distribution of concentrations of basic components across the boundary layer. The ordinate here is the molar fraction of the i-component, y_i. Two characteristic zones are observed in the boundary layer. The first, of extent 2 mm, lies close to the wall of the disintegrating material and has a constant temperature. Here the concentration of disintegration products varies very little. A second zone, located in the high-temperature region, relates to the outer edge of the boundary layer, and is characterized by a sharp fall in the concentrations of all the components.

In regard to the variation of vapor concentration across the boundary layer, the components can be divided into three groups. The curves referring to variations of Ca, Na, K with excitation potential $E_n \sim 2$-4 eV have a maximum concentration at the wall and decrease sharply toward the outer edge. The concentrations of the atoms Al, Fe, Mg, Si, and Mn, with excitation potential $E_n \sim 3$-5 eV, have a maximum in a layer $\sim$1 mm distant from the wall. The CN radical belongs to this group. The concentration of carbon, measured from the CI 2478-Å line with excitation potential $\sim$8 eV, has a maximum displaced toward the high-temperature region. The third group contains the molecular components C_2, SiO, MgO, AlO, and CaO, whose concentrations cannot be measured because of the disturbances introduced by the side lines in their rotational structure. However, it should be noted that the radiative spectra of these compounds are observed at the disintegrating wall in layers of thickness $\sim$0.5-2 mm, i.e., the maximum of luminous intensity, and, therefore, the maximum concentration is found at the outer edge of the boundary layer. We can deduce that these compounds are formed because of sublimation of the corresponding oxides of the melt of superheated material. Thus, near the wall the boundary-layer composition is mainly determined by the products of disintegration of the material.

We have compared the experimental data with theory, shown by dashed lines in Fig. 4, for the elements Mg and C. The calculation was performed for an equilibrium, chemically reacting system, without allowance for interaction of the original asbestos material with the heated air. This comparison makes sense only for the wall region, consisting mainly of the disintegration products of the material, for which, as can be seen from Fig. 4, good agreement with theory is observed.

Thus, we can assert that the wall region of the thermal boundary layer holds promise for the study of spectral absorption coefficients, since the temperature, pressure, and chemical composition are sufficiently constant there.

NOTATION

V, velocity; t, time; Q, effective collisional cross section; z, number of collisions; Z, statistical sum for the electronic, vibrational, and rotational states of the molecule; ν_{UX}, electronic transition frequency; N, total number of molecules in 1 cm^3; l, length of the radiating layer; $|R_e^{UX}|^2$, matrix element for the electronic transition; $q_{v'v''}$, Frank—Condon factor; $S_{K'K''}$, Hönl—London factor; c, speed of light; k, Boltzmann constant; T, temperature; E_U, $E_{v'}$, $E_{K'}$, energy of the upper electronic, vibrational, and rotational levels; v', v", K', K", vibrational and rotational numbers in the upper and lower electronic states; y_i, molar fraction of the i-th component; E_n, excitation energy; I, radiative intensity.

LITERATURE CITED

1. Yu. P. Raizer, Zh. Prikl. Mekh. Tekh. Fiz., No. 3 (1968).
2. É. B. Georg, Yu. K. Rulev, and M. I. Yakushin, Izv. Akad. Nauk SSSR, Mekh. Zhidk. Gaza, No. 5 (1973).
3. É. B. Georg and M. I. Yakushin, Izv. Akad. Nauk SSSR, Mekh. Zhidk. Gaza, No. 1 (1976).
4. E. M. Kudryavtsev, Tr. Fix. Inst. Akad. Nauk SSSR, 35, (1966), 74 (1966).
5. R. W. Nicholls, Proc. Phys. Soc., Ser. A, 69, No. 10 (1956).
6. V. A. Kamenshchikov, Yu. A. Plastinin, V. M. Nikolaev, and L. A. Novitskii, Radiative Properties of High-Temperature Gases [in Russian], Mashinostroenie, Moscow (1971).
7. N. N. Thomas, J. Chem. Phys., 20, No. 3 (1952).
8. L. V. Leskov and L. P. Vasil'eva, Izv. Akad. Nauk SSSR, Ser. Fiz., 22, No. 6 (1958).
9. R. G. Bennet and F. W. Dalby, J. Chem. Phys., 36, No. 2 (1962).
10. A. N. Zaidel', V. K. Prokof'ev, S. M. Raiskii, and E. Ya. Shreider, Tables of Spectral Lines [in Russian], FM, Moscow (1962).
11. W. I. Wiese et al., Atomic Transition Probabilities, Vol. 2, NBS (1969).
12. C. Korliss and U. Bozman, Transition Probabilities and Oscillator Strengths for 70 Elements [Russian translation], Mir, Moscow (1968).